Absolute calibration of gravitational wave detector using gravity field and photon pressure

Yuki Inoue[a,b], Sadakazu Haino[a], Nobuyuki Kanda[c], Yujiro Ogawa[b.d], Toshikazu Suzuki[b,e], Takayuki Tomaru[b,d,e], Takahiro Yamamoto[f], Takaaki Yokozawa[f]

[a]Institute of Physics, Academia Sinica, Nankang, Taipei 11529, Taiwan;
[b]High Energy Accelerator Research Organization, Tsukuba, Ibaraki, 305-0801, Japan;
[c]Department of Physics, Osaka City University, Sumiyoshi, Osaka 558-8585, Japan;
[d]SOKENDAI (The Graduate University for Advanced Studies), Hayama, Miura District, Kanagawa 240-0115, Japan;
[e]Institute for Cosmic Ray Research, University of Tokyo, Kashiwa, Chiba, 277-8582, Japan;
[f]KAGRA Observatory, Institute for Cosmic Ray Research, University of Tokyo, Hida, Gifu 506-1205, Japan;

ABSTRACT

Absolute calibration of the gravitational wave detectors is an essential to evaluate the various parameters of the gravitational wave sources. The photon calibrator is primary calibrator for calibrating the absolute displacement of the mirror by using the photon pressure. Current technological limit of the absolute calibration uncertainty is 3.5 % corresponding to the uncertainty of the laser power standard of the standard metrology institutes from nine country. In order to reduce the uncertainty of the photon calibrator, we propose a new method using the combination of photon calibrator and gravity field calibrator. The gravity field calibrator gives the modulation to mirror using the gravity gradient. In previous study, uncertainty of the distance between the test mass and gravity field calibrator is one of the serious systematic error of the absolute calibration. To cancel this uncertainty, we newly propose the method of quadrupole and hexapole mass distribution. We also estimated the uncertainty of this method. The estimated precision of absolute calibration is 0.3%, which is 10 times less than that of previous method.

Keywords: Gravitational Wave, KAGRA, LIGO, Virgo, Calibration

1. INTRODUCTION

The discovery of the gravitational wave (GW) gave us the new probe for observing our universe.[1] The typical strain sensitivity, h, of 2nd generation interferometric detectors (IFO), such as Advanced LIGO,[2] Advanced Virgo,[3] and KAGRA,[4,5] are around $10^{-23}/\sqrt{Hz}$ at 100 Hz. By using the GW signals from compact binary coalescences, we can derive the parameters such as masses, spins, luminosity distance, orbital inclination and the sky location of the binary system from the detected waveforms. The precision of the derived parameters are potentially limited by the calibration accuracy. As the number of detected sources increases and we detect higher signal-to-noise ratio (SNR) events, the calibration uncertainty will become the dominant source of the errors to extract physics information. In particular, the uncertainty on the absolute GW signal amplitude directly propagates to the error on the estimation of the distance to the sources. The detection of GW signal from a Binary Neutron Star (BNS) system, GW170817[6] in both GW and Electro-Magnetic (EM) waves opened a new era of multi-messenger astronomy. These observations allow us to use GW170817 as a standard siren[7–10] to determine the absolute luminosity distance to the source directly from the GW signal measurements. Assuming the event rate of 3000 $\mathrm{Gpc^{-3}yr^{-1}}$ which is consistent with the bounds from GW170817 at 90% confidence,[6] we expect to detect GW signals from about 50 BNS standard sirens in the next few observing runs. They can constrain the Hubble constant (H_0) measurement to 2% or less,[11] and eventually resolve the 3-σ tension of the H_0 measurement between Cephied-SN distance ladder[12] and CMB data assuming a ΛCDM model.[13] The

Yuki Inoue: iyuki@post.kek.jp

systematic errors on the calibration of the absolute GW signal amplitude must be suppressed at the sub-% level to achieve the high precision H_0 measurement with the GW standard sirens.

An interferometer measures the change of distance difference along the two arms of interferometer. Then, the fluctuations in the degree of freedom of differential arm length (DARM) is suppressed by the DARM control loop. The reconstruction signal of DARM fluctuation at the observation frequency is excited by the gravitational waves. We can reconstruct the gravitational waveform with the calibrated error and control signals of this DARM loop. To calibrate the signals, the accurate modelings of the actuator and sensing function are essential. To understand the model, we need to measure the transfer function and monitor the time dependency of the transfer function using continuous sine curve (calibration lines). The residual of the time-dependent models corresponds to uncertainty of the detection.

To reduce the calibration systematic uncertainty, we need to inject well parameterized calibration line by photon calibrator (Pcal) or other calibration source for monitoring the time variation of the response of IFO. The first generation of the photon calibrator was developed by the Glasgow and GEO600.[14,15] They proposed the modulation method with photon pressure for understanding the response of interferometer. The second generation photon calibrator is developed by LIGO.[3,16–18] LIGO and Virgo employ the second generation photon calibrator for the calibration of time-dependent response of IFO.[3] The third generation photon calibrator is developed by KAGRA.[19] KAGRA employ the 20 W laser and independent modulation system for injected beams. LIGO and KAGRA use a power sensor called to as the Gold standard, which is calibrated by the laser power standard of NIST in Boulder, CO.[20] However, it has a challenging issue of the absolute calibration due to the accuracy of the absolute laser power of laser standard between national metrology institute from nine countries. The systematic discrepancies between nine countries are as large as 3.5 %.[21]

The dynamic gravity field calibrator (Gcal) is one of the candidates to be able to solve the uncertainty problem of absolute calibration. The technologies of the system are established and tested in Forward and Miller,[22] Weber,[23,24] University of Tokyo[25–29] and Rome university group.[30] Related techniques using gravity field calibrator for the calibration are discussed in Matone et al.[31] It can modulate the test mass using gravity gradient with rotor. The amplitude of displacement of the mirror is determined by masses, distance, frequency, radius, and gravity constant.

In this paper, we propose how we can achieve sub-percent uncertainty of the calibration. We focus on the combination method of the photon calibrator and gravity field calibrator. In section 2, we explain how to calibrate with photon calibrator. In chapter 3, we show the principle of multipole moment gravity and modulation method. In section 4, we show how to calibrate the absolute displacement with Pcal and Gcal. In section 5, we discuss the systematic error by changing parameters.

2. PHOTON CALIBRATOR

Pcal relies on the photon radiation pressure from the power modulated laser beams reflecting on the test mass to apply periodic force via the recoil of photons.[16] advanced LIGO, advanced Virgo and KAGRA employ the photon calibrator for the calibration of the interferometer response.[3,19,32] Each gravitational detectors placed the 1047 nm laser around the end test mass. The displacement of the test mass can be described as

$$x = \frac{P\cos\theta}{2c} s(\omega) \left(1 + \frac{M}{I}\vec{a}\cdot\vec{b}\right), \tag{1}$$

where P is absolute laser power, θ is incident angle of the Pcal laser, M is mass of test mass, ω is angular frequency of the laser power modulation, $\vec{a}$ and $\vec{b}$ are position vector of Pcal laser beams. The schematic view is shown in Fig. 1. $I = Mh^2/12 + Mr^2/4$ is the moment of inertia, where h and r are thickness and radius of test mass. $s(\omega)$ is transfer function between force and displacements. We can regard the $s(\omega)$ as $1/(M\omega^2)$ above 20 Hz.

The laser power is stabilized less than design sensitivity. The schematic view of the photon calibrator is shown in Fig. 1. The stabilized laser is mounted on the transmitter module. The power is monitored by the response of the photo detectors at the transmitter module, V_{TxPD}, and receiver module, V_{RxPD}. The largest relative uncertainty of photon calibrator is that of laser power. LIGO and KAGRA use the working standard

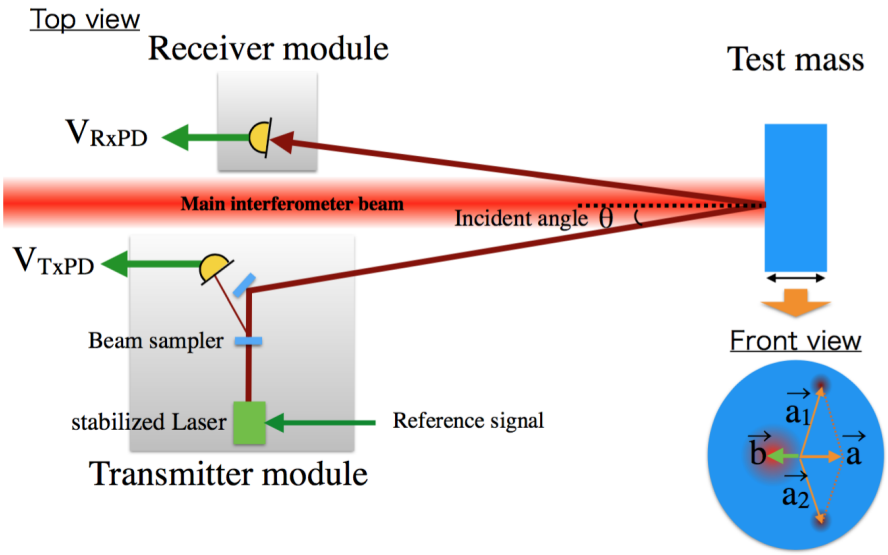

Figure 1. Schematic view of photon calibrator. We place the stabilized laser on the transmitter module. The injected signal at the test masses is monitored by using the response of photo detector power between the transmitter module, V_{TxPD} and receiver module, V_{RxPD}. The geometrical factor is characterized by the position vectors of photon calibrator beams, $\vec{a} = \vec{a_1} + \vec{a_2}$, and the main beam, $\vec{b}$.

Table 1. Specification summary of LIGO, Virgo and KAGRA photon calibrator

	KAGRA	advanced LIGO	advanced Virgo
Mirror material	Sapphire	Silica	Silica
Mirror mass	23 kg	40 kg	40 kg
Mirror diameter	220 mm	340 mm	350 mm
Mirror thickness	150 mm	200 mm	200 mm
Distance of Pcal from ETM	36 m	8 m	1.5 m
Pcal laser power	20 W	2W	3 W
Pcal laser frequency	1047 nm	1047 nm	1047 nm
Incident angle	0.72 deg	8.75 deg	30 deg

to cross-calibrate the relative response of each interferometer. The relative uncertainty of each calibrator is 0.51 %.[16] The second largest relative uncertainty is an optical efficiency of the optical path. We calibrate the injected power from the outside of the vacuum chamber. Therefore, we need to consider the optical efficiency due to the transmittance of the vacuum window and reflectance of the mirrors. The measured uncertainty of optical efficiency in LIGO is 0.37 %. For the absolute calibration, the detector, so called "Gold standard", is calibrated with the NIST laser power standard. After that, The responses of "Working standard" of Hanford, Livingston and KAGRA are calibrated by the "Gold standard" in LIGO Hanford observatory. However, the result of comparison between accuracies of the absolute laser powers of each institutes has 3.5 % uncertainty. It implies that the serious systematic error for distance estimation because the uncertainty of the absolute calibration propagate to the distance of the GW source.

3. GRAVITY FIELD CALIBRATOR

To solve the uncertainty problem of the absolute calibration, we propose the method of gravity field calibrator. The gravity field calibrator generate the dinamic gravity field at the end of test mass by rotating the multipole masses. The rotor placed in the vacuum chamber for isolating the acoustic noise. To monitor the frequency, we mount the 10-bit encoder. We read the response of encoder using 16 bit ADC system. We calculated the displacement by changing dynamic gravity field of multipole moment with N peaces of masses. We assumed

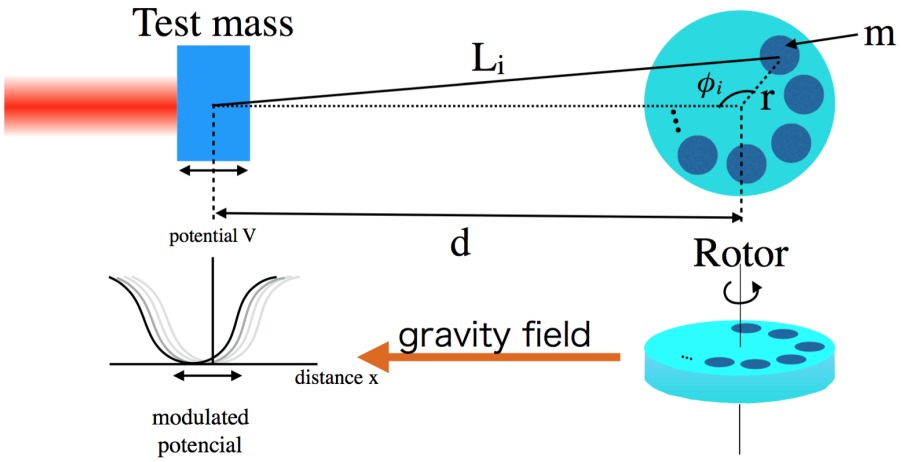

Figure 2. Schematic view of gravity field calibrator. We placed the rotor at the same hight and the distance of d away from test masses. Multipole mass generate the gravitational potential at the test mass position.

the suspended test mass for the interferometer and disk with multipole masses as shown in Fig 2. We put the masses, m, at the positions of the radius, r. The distance between the center of mass of mirror and disk is assumed d. We rotate the disk at the angular frequency of $\omega_{\rm rot} = 2\pi f_{\rm rot}$.

First we calculate the distance with N pieces of masses which are separated by radius of r from the center of the rotor mass and arranged at equal intervals, respectively. Distance between i-th mass and center of test mass is written as

$$L_i = d\sqrt{1 + \left(\frac{r}{d}\right)^2 - 2\left(\frac{r}{d}\right)\cos\phi_i}, \tag{2}$$

where the angle of i-th mass is assumed as $\phi_i = \omega_{\rm rot}t + 2\pi i/N$. The gravity potential at the center of test mass can be described as

$$\begin{aligned} V &= \Sigma_{i=0}^{N} V_i & (3)\\ &= -GMm\Sigma_{i=0}^{N} L_i^{-1} & (4)\\ &= -\frac{GMm}{d}\Sigma_{i=0}^{N}\Sigma_{n=0}^{\infty}\left(\frac{r}{d}\right)^n P_n\left(\cos\left(\omega_{\rm rot}t + \frac{2\pi i}{N}\right)\right), & (5) \end{aligned}$$

where P_n is Legendre polynomial, and V_i is potential of a mass. The equation of motion of test mass is

$$Ma = \left|\frac{\partial V}{\partial d}\right| = \frac{GMm}{d^2}\Sigma_{i=0}^{N}\Sigma_{n=0}^{\infty}(n+1)\left(\frac{r}{d}\right)^n P_n\left(\cos\left(\omega_{\rm rot}t + \frac{2\pi i}{N}\right)\right), \tag{6}$$

where a is acceleration of test mass.

We place the quadrupole and hexapole masses in the same rotor as shown in Fig. 3. We put the hole between each mass. The hole can increase the gravity gradient twice effectively. Therefore, we can describe the equation of motion as

$$Ma = \left|\frac{\partial V}{\partial d}\right| = \frac{2GMm}{d^2}\Sigma_{i=0}^{N}\Sigma_{n=0}^{\infty}(n+1)\left(\frac{r}{d}\right)^n P_n\left(\cos\left(\omega_{\rm rot}t + \frac{2\pi i}{N}\right)\right). \tag{7}$$

We will calculate the displacement of quadrupole and hexapole in the section 3.1 and 3.2.

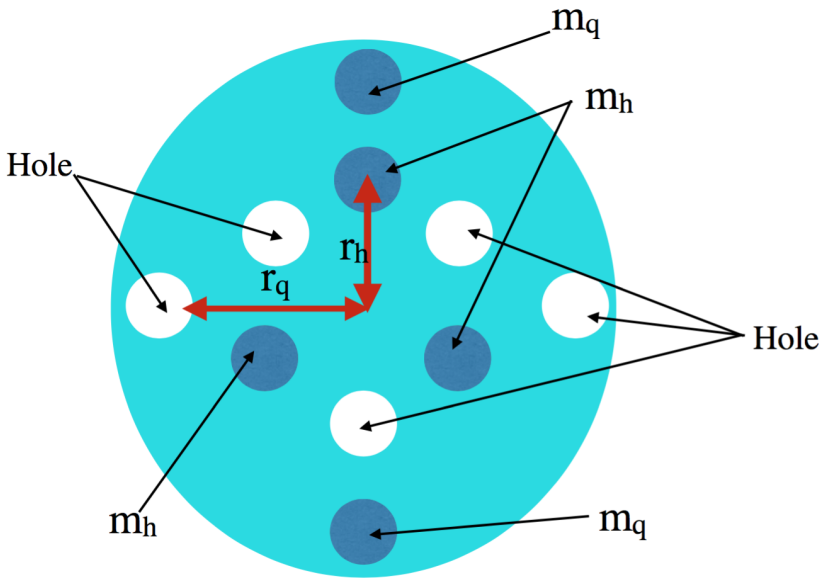

Figure 3. Configuration of the rotor with quadrupole and haxapole mass distribution. $m_{\rm q}$ and $m_{\rm h}$ are mass of quadrupole and hexapole. $r_{\rm q}$ and $r_{\rm h}$ are radius of quadrupole and hexapole.

3.1 Displacement of test mass (Quadrupole)

We calculate the displacement of the quadrupole mass distribution corresponding to $N = 2$. The masses and radiuses of quadrupole are assumed as $m_{\rm q}$ and $r_{\rm q}$. The equation of motion of test mass is described as

$$Ma = \frac{2GMm_{\rm q}}{d^2}\Sigma_{n=0}^{\infty}(n+1)\left(\frac{r_{\rm q}}{d}\right)^n \left(P_n\left(\cos\left(\omega_{\rm rot}t\right)\right) + P_n\left(\cos\left(\omega_{\rm rot}t+\pi\right)\right)\right). \tag{8}$$

If we assume $r \ll d$, the displacement of the time-dependent lower harmonics can be written by

$$x = \Sigma_{k=1}^{\infty} x_{kf}\cos(k\omega_{\rm rot}t) \sim x_{2f}\cos(2\omega_{\rm rot}t) = x_{2f}\cos\omega t, \tag{9}$$

where k is the number of the harmonics. The amplitude of 2-f rotation is described as

$$x_{2f} = 9\frac{GMm_{\rm q}r_{\rm q}^2}{d^4}s(\omega). \tag{10}$$

3.2 Displacement of test mass (Haxapole)

We also calculate the displacement of the hexapole mass distribution, which corresponds to $N = 3$. The masses and radiuses of hexapole are assumed as $m_{\rm h}$ and $r_{\rm h}$. The equation of motion of test mass is described as

$$\begin{aligned} Ma \quad = \quad & \frac{2GMm_{\rm h}}{d^2}\Sigma_{n=0}^{\infty}(n+1)\left(\frac{r_{\rm h}}{d}\right)^n \\ & \times\left(P_n\left(\cos\left(\omega_{\rm rot}t\right)\right) + P_n\left(\cos\left(\omega_{\rm rot}t+\frac{2\pi}{3}\right)\right) + P_n\left(\cos\left(\omega_{\rm rot}t\frac{4\pi}{3}\right)\right)\right). \end{aligned} \tag{11}$$

If we assume $r \ll d$, the displacement of the time-dependent lower harmonics can be written by

$$x = \Sigma_{k=1}^{\infty} x_{kf}\cos(k\omega_{\rm rot}t) \sim x_{3f}\cos(3\omega_{\rm rot}t) = x_{3f}\cos\omega t, \tag{12}$$

where amplitude of 3-f is described as

$$x_{3f} = 15\frac{GMm_{\rm h}r_{\rm h}^3}{d^5}s(\omega). \tag{13}$$

4. ABSOLUTE POWER CALIBRATION BY USING GCAL AND PCAL

In this section, we discuss about absolute laser power calibration using interferometer. Figure 4 shows the configuration of the calibration by using the combination of photon calibrator and gravity field calibrator. First, we modulate the mirror position using gravity field calibrator. We can measure the signal of $x_{2\mathrm{f}}$ and $x_{3\mathrm{f}}$ in the response of interferometer. Second, we send the interferometer signal to the excitation port of photon calibrator as a reference signal port of feedback control as shown in Fig. 4. The photon calibrator cancel the displacement by gravity field calibrator. Third, we measure the response of the detector of transmitter module and receiver module, whose units are volt. The output signal of transmitter module, V_{TxPD} and receiver module, V_{RxPD} should be corresponding to displacement from gravity field. By using Eq (1),(10), and (13), the modulated powers are

$$P_{2\mathrm{f}} = 18\frac{Gcm_{\mathrm{q}}Mr_{\mathrm{q}}^2}{d^4 cos\theta}\frac{1}{1+\frac{M}{I}\vec{a}\cdot\vec{b}} \tag{14}$$

$$P_{3\mathrm{f}} = 30\frac{Gcm_{\mathrm{h}}Mr_{\mathrm{h}}^3}{d^5 cos\theta}\frac{1}{1+\frac{M}{I}\vec{a}\cdot\vec{b}} \tag{15}$$

Fourth, we demodulate the signal of the transmitter and receiver modules using the measured encoder signal of gravity field calibrator. The demodulated signals are

$$V_{2\mathrm{f}}^{\mathrm{T}} = \rho_{\mathrm{T}}P_{2\mathrm{f}}, \tag{16}$$

$$V_{2\mathrm{f}}^{\mathrm{R}} = \rho_{\mathrm{R}}P_{2\mathrm{f}}, \tag{17}$$

$$V_{3\mathrm{f}}^{\mathrm{T}} = \rho_{\mathrm{T}}P_{3\mathrm{f}}, \tag{18}$$

$$V_{3\mathrm{f}}^{\mathrm{R}} = \rho_{\mathrm{R}}P_{3\mathrm{f}}, \tag{19}$$

where ρ_{T} and ρ_{R} are transfer function from power to voltage of the photo detector output at the transmitter and receiver modules. Therefore, we can measure the distance with the ratio of response between 2-f and 3-f components:

$$d = \frac{5}{3}\frac{V_{2\mathrm{f}}^{\mathrm{T}}}{V_{3\mathrm{f}}^{\mathrm{T}}}\frac{m_{\mathrm{h}}}{m_{\mathrm{q}}}\frac{r_{\mathrm{h}}^3}{r_{\mathrm{q}}^2} = \frac{5}{3}\frac{V_{2\mathrm{f}}^{\mathrm{R}}}{V_{3\mathrm{f}}^{\mathrm{R}}}\frac{m_{\mathrm{h}}}{m_{\mathrm{q}}}\frac{r_{\mathrm{h}}^3}{r_{\mathrm{q}}^2}. \tag{20}$$

Finally, we insert the equatin (10) to the Eq. (1):

$$x = \frac{P\cos\theta}{2c}s(\omega)\left(1+\frac{M}{I}\vec{a}\cdot\vec{b}\right) \tag{21}$$

$$= 9\frac{P}{P_{2\mathrm{f}}}\frac{Gm_{\mathrm{q}}Mr_{\mathrm{q}}^2}{d^4}s(\omega), \tag{22}$$

$$= \frac{729}{625}\frac{Gm_{\mathrm{q}}^5 r_{\mathrm{q}}^{10}}{m_{\mathrm{h}}^4 r_{\mathrm{h}}^{12}\omega^2}\frac{V_{3\mathrm{f}}^{R^4}}{V_{2\mathrm{f}}^{R^5}}V_{\mathrm{in}}, \tag{23}$$

where we assume $P(\omega) = \rho_{\mathrm{R}}V_{\mathrm{in}}$, and V_{in} is amplitude of the input voltage.

5. ESTIMATION OF UNCERTAINTY

In evaluating the accuracy of the estimated displacement, we discuss the systematic error by changing the operation frequency and distance. After that, we discuss the uncertainty of the displacement of the mirror. We estimate the uncertainty of the displacement by assuming KAGRA basic parameter as shown in Fig. 1. The assumed parameters of the calibrators are listed in Table 2. We assumed these number in the following section.

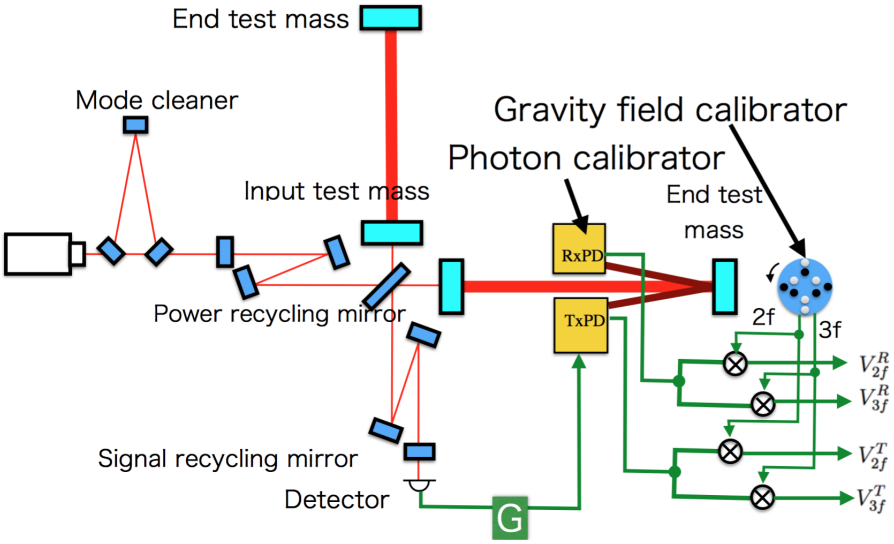

Figure 4. Test setup of the calibration of the laser power by rotating gravity field calibrator.

Table 2. The assumed parameters.

		Value	Relative uncertainty
G	Gravity constant	6.6742×10^{-11} [m^{3}kg^{-1}sec^{-2}]	0.015 %
$\cos\theta$	Incident angle	1.000	0.07 %
M	Mass of test mass	22.89 [kg]	0.02 %
$m_{\rm q}$	Mass of quadrupole	4.485 [kg]	0.004 %
$m_{\rm h}$	Mass of hexapole	4.485 [kg]	0.004 %
$r_{\rm q}$	Radius of quadrupole	0.200 [m]	0.01 %
$r_{\rm h}$	Radius of hexapole	0.125 [m]	0.02 %
$1+\frac{I}{M}\vec{a}\cdot\vec{b}$	Geometrical factor	1	0.3 %

5.1 Systematic error of the higher order term

In order to achieve the precision less than 1 %, we need to consider the operation position due to the higher order of Legendre polynomial. This is because that higher order also include the 2-f and 3-f components. The order of the Legendre polynomial is characterized by n as shown in Eq.(7). The effect of higher order factor is mitigated by the factor of $(r/d)^n$. Table 3 and 4 shows the calculated displacement of the higher order term. To compare the higher order effect, we calculate the ratio between the FEM and calculation by changing the r/d is shown in Fig 5. We need to place the mirror at least 2 m away from the mirror to reduce the systematic error. In the following calculation, we assume the distance as 2 m.

Table 3. The calculated quadrupole($N=2$) displacement. n is order of Legendre polynomial, where $\omega = n\omega_{\rm rot}$.

modulation	n=1	n=2	n=3	n=4	n=5	n=6	n=7
1f	0	0	0	0	0	0	0
2f	0	$9\frac{Gmr^2}{d^4\omega^2}$	0	$\frac{25}{4}\frac{Gmr^4}{d^6\omega^2}$	0	$\frac{735}{128}\frac{Gmr^6}{d^8\omega^2}$	0
3f	0	0	0	0	0	0	0
4f	0	0	0	$\frac{175}{16}\frac{Gmr^4}{d^6\omega^2}$	0	$\frac{441}{64}\frac{Gmr^6}{d^8\omega^2}$	0
5f	0	0	0	0	0	0	0
6f	0	0	0	0	0	$\frac{1617}{128}\frac{Gmr^6}{d^8\omega^2}$	0

Table 4. The calculated hexapole($N = 3$) displacement. n is order of Legendre polynomial, where $\omega = n\omega_{\rm rot}$.

modulation	n=1	n=2	n=3	n=4	n=5	n=6	n=7
1f	0	0	0	0	0	0	0
2f	0	0	0	0	0	0	0
3f	0	0	$15\frac{Gmr^3}{d^5\omega^2}$	0	$\frac{315}{32}\frac{Gmr^5}{d^7\omega^2}$	0	$\frac{189}{64}\frac{Gmr^7}{d^9\omega^2}$
4f	0	0	0	0	0	0	0
5f	0	0	0	0	0	0	0
6f	0	0	0	0	0	$\frac{4851}{256}\frac{Gmr^6}{d^8\omega^2}$	0

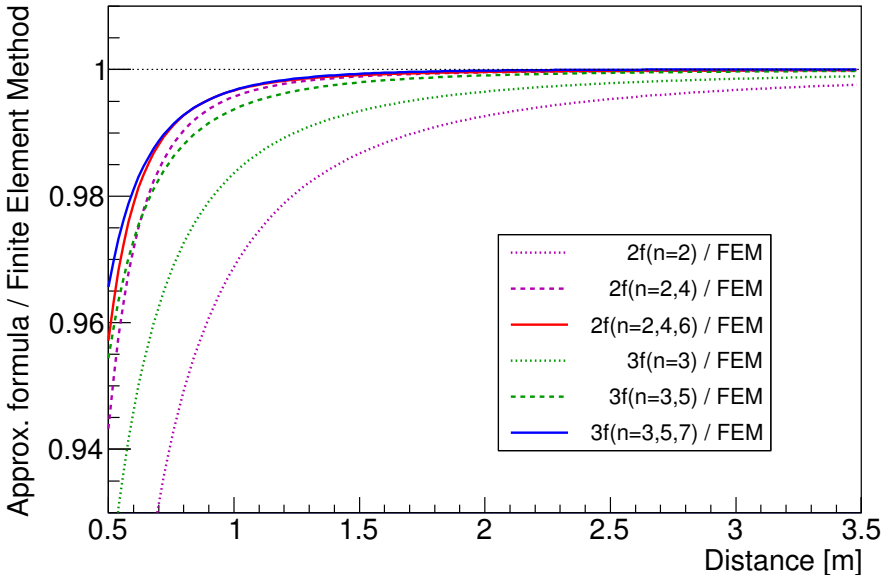

Figure 5. The displacement ratio of the higher order effect by changing r/d. Dashed curves are included with the 1st order term. Solid curves are included with sum of 1st order and 2nd order. The analytical result is listed in Table 3 and 4. To achieve the precision less than 1 %, we need include the higher order terms.

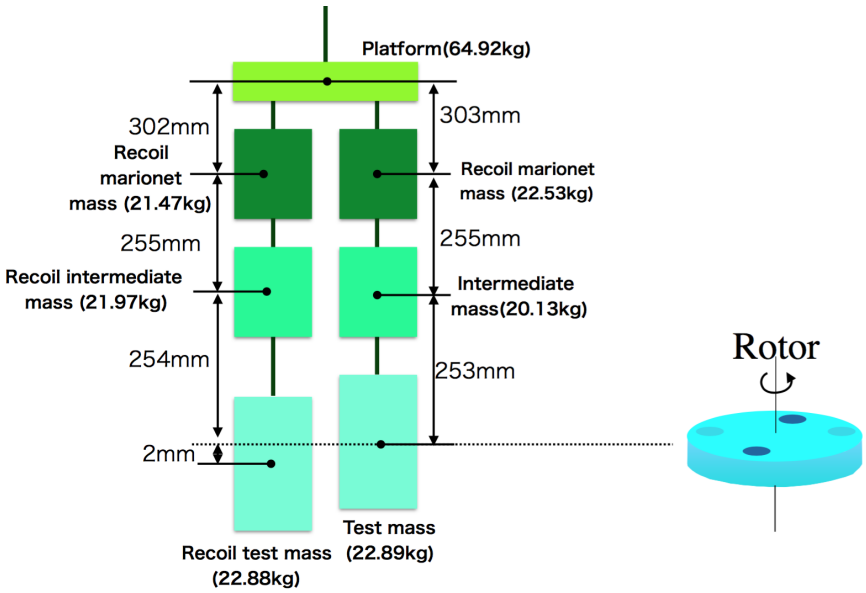

Figure 6. Schematic view of the suspension system. The parameter of the hight and mass is the assumed value.

5.2 Systematic error of the transfer function

The gravity field calibrator can modulate the mirrors with gradient of gravity potential. However, its gravity gradient act the masses of suspension system as shown in Fig. 6. We simulated the transfer function between each mass and test mass.The transfer function is calculated by the suspension rigid-body simulation code, called SUMCON.[?] We estimated the total displacement including all the masses. Figure 7 shows the displacement ratio between the sensed motion and free mass motion as a function of frequency The structures of low frequency are corresponding to the resonant peak of the suspension system. We can neglect the intermediate mass effect and regard as free mass motion larger than 10 Hz. We assumed the rotation frequency as 16 Hz, which is corresponding to 32 Hz and 48 Hz at the operation frequency. of 2-f and 3-f components. We used this assumption in the following section.

5.3 Uncertainty of displacement and laser power

In this section, we estimate the typical displacement based on the Table. 2. The estimated displacements of 2-f and 3-f are described as

$$x_{\rm 2f}^{\rm rms} = 1.178\times10^{-16}[{\rm m}]\times\left(\frac{G}{6.6742\times10^{-11}[{\rm m^3kg^{-1}sec^{-2}}]}\right)\times\left(\frac{m_{\rm q}}{4.485[{\rm kg}]}\right)\times\left(\frac{r_{\rm q}}{0.200[{\rm m}]}\right)^2 \times\left(\frac{2[{\rm m}]}{d}\right)^4\times\left(\frac{2\pi(2\times16)[{\rm Hz}]}{\omega}\right)^2 \tag{24}$$

$$x_{\rm 3f}^{\rm rms} = 2.130\times10^{-18}[{\rm m}]\times\left(\frac{G}{6.6742\times10^{-11}[{\rm m^3kg^{-1}sec^{-2}}]}\right)\times\left(\frac{m_{\rm h}}{4.485[{\rm kg}]}\right)\times\left(\frac{r_{\rm h}}{0.125[{\rm m}]}\right)^3 \times\left(\frac{2[{\rm m}]}{d}\right)^5\times\left(\frac{2\pi(3\times16)[{\rm Hz}]}{\omega}\right)^2. \tag{25}$$

We defined the signal-to-noise ratio (SNR) with the ratio of RMS displacement to the design noise spectrum density of IFO of KAGRA at 32 Hz for 2-f and 48 Hz for 3-f. By using this result, we estimate the signal to noise ratio of the peaks.

$$SNR_{\rm 2f} = 392\times\left(\frac{3.0\times10^{-19}{\rm m}/\sqrt{\rm Hz}}{n_{\rm 32Hz}}\right)\times\left(\frac{T}{1[{\rm sec}]}\right)^{1/2}\times\left(\frac{x_{\rm 2f}^{\rm rms}}{1.178\times10^{-16}[{\rm m}]}\right), \tag{26}$$

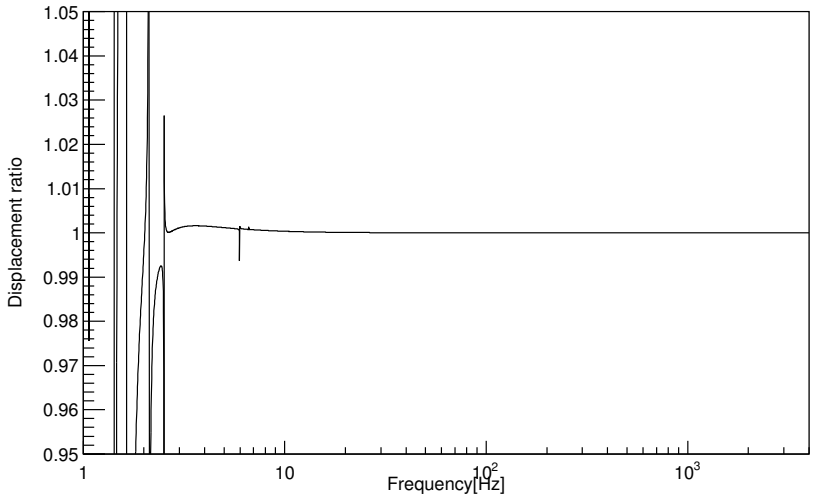

Figure 7. The displacement ratio of the transfer function of multi pendulum by changing modulation frequency, where relations of the modulation frequency, f, modulation angular frequency, ω, and rotation angular frequency, $\omega_{\rm rot}$ are described as. $n\omega_{\rm rot} = \omega = 2\pi f$. If we put the gravity field calibrator, it act the upper masses and it makes systematic error of the transfer function.

$$SNR_{3\rm f} = 73 \times \left(\frac{2.9 \times 10^{-20}{\rm m}/\sqrt{\rm Hz}}{n_{48\rm Hz}} \right) \times \left(\frac{T}{1[\rm sec]} \right)^{1/2} \times \left(\frac{x_{2\rm f}^{\rm rms}}{2.130 \times 10^{-18}[\rm m]} \right) \tag{27}$$

$$\tag{28}$$

where T is integration time. When we integrate the signal larger than 10 min, we can measure the $V_{2f}^{\rm R}$ and $V_{3f}^{\rm R}$ with enough of SNR. We can apply this system for the measurement of the absolute laser power. The estimated powers are

$$\begin{aligned} P_{2\rm f} &= 0.09288\ [\rm W] \times \left(\frac{G}{6.6742 \times 10^{-11}[\rm m^3 kg^{-1} sec^{-2}]} \right) \\ &\quad \times \left(\frac{m_{\rm q}}{4.485[\rm kg]} \right) \times \left(\frac{r_{\rm q}}{0.200[\rm m]} \right)^2 \times \left(\frac{2[\rm m]}{d} \right)^4 \times \left(\frac{1}{\cos\theta} \right) \times \left(\frac{1}{1 + \frac{M}{I}\vec{a}\cdot\vec{b}} \right)^2 \end{aligned} \tag{29}$$

$$\begin{aligned} P_{3\rm f} &= 0.003779\ [\rm W] \times \left(\frac{G}{6.6742 \times 10^{-11}[\rm m^3 kg^{-1} sec^{-2}]} \right) \\ &\quad \times \left(\frac{m_{\rm h}}{4.485[\rm kg]} \right) \times \left(\frac{r_{\rm h}}{0.125[\rm m]} \right)^3 \times \left(\frac{2[\rm m]}{d} \right)^5 \times \left(\frac{1}{\cos\theta} \right) \times \left(\frac{1}{1 + \frac{M}{I}\vec{a}\cdot\vec{b}} \right)^2 . \end{aligned} \tag{30}$$

The estimated $V_{2\rm f}^{\rm T}/V_{3\rm f}^{T}$ by changing distance are shown in Fig. 8.

We can also estimate the laser power by using the following equations:

$$\begin{aligned} \left(\frac{\delta P_{2\rm f}}{P_{2\rm f}} \right)^2 &\sim \left(\frac{\delta G}{G} \right)^2 + \left(\frac{\delta M}{M} \right)^2 + 25 \left(\frac{\delta m_{\rm q}}{m_{\rm q}} \right)^2 + 16 \left(\frac{\delta m_{\rm h}}{m_{\rm h}} \right)^2 + 100 \left(\frac{\delta r_{\rm q}}{r_{\rm q}} \right)^2 + 144 \left(\frac{\delta r_{\rm h}}{r_{\rm h}} \right)^2 \\ &+ 16 \left(\frac{\delta V_{2\rm f}^{\rm R}}{V_{2\rm f}^{\rm R}} \right)^2 + 16 \left(\frac{\delta V_{2\rm f}^{\rm R}}{V_{2\rm f}^{\rm R}} \right)^2 + \left(\frac{\delta(\cos\theta)}{\cos\theta} \right)^2 + \left(\frac{\delta\left(1 + \frac{M}{I}\vec{a}\cdot\vec{b}\right)}{\left(1 + \frac{M}{I}\vec{a}\cdot\vec{b}\right)} \right)^2 \end{aligned} \tag{31}$$

$$\left(\frac{\delta P_{3\rm f}}{P_{3\rm f}} \right)^2 \sim \left(\frac{\delta G}{G} \right)^2 + \left(\frac{\delta M}{M} \right)^2 + 25 \left(\frac{\delta m_{\rm q}}{m_{\rm q}} \right)^2 + 16 \left(\frac{\delta m_{\rm h}}{m_{\rm h}} \right)^2 + 100 \left(\frac{\delta r_{\rm q}}{r_{\rm q}} \right)^2 + 144 \left(\frac{\delta r_{\rm h}}{r_{\rm h}} \right)^2$$

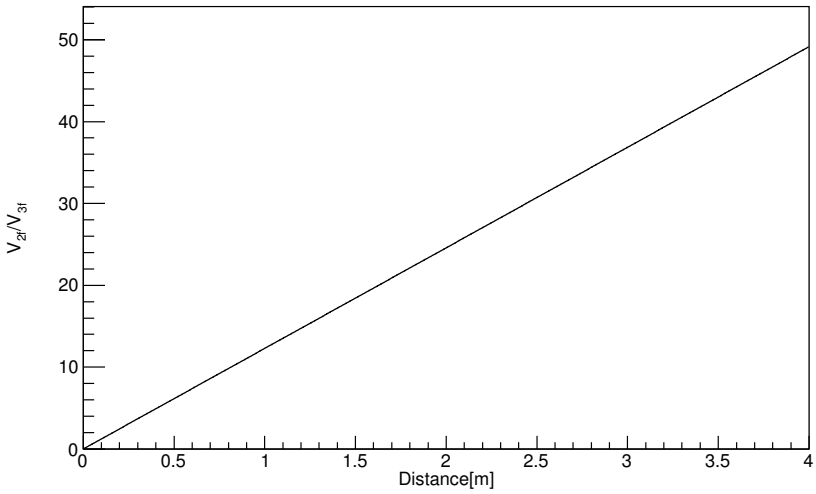

Figure 8. The response of $V_{2\mathrm{f}}/V_{3\mathrm{f}}$ by changing distance between test mass and gravity field calibrator.

$$+ \quad 16\left(\frac{\delta V_{2\mathrm{f}}^{\mathrm{R}}}{V_{2\mathrm{f}}^{\mathrm{R}}}\right)^2 + 16\left(\frac{\delta V_{2\mathrm{f}}^{\mathrm{R}}}{V_{2\mathrm{f}}^{\mathrm{R}}}\right)^2 + \left(\frac{\delta(\cos\theta)}{\cos\theta}\right)^2 + \left(\frac{\delta\left(1+\frac{M}{I}\vec{a}\cdot\vec{b}\right)}{\left(1+\frac{M}{I}\vec{a}\cdot\vec{b}\right)}\right)^2 \tag{32}$$

The uncertainty of the quadrupole and hexapole masses are limited by the accuracy of electronic balance. In this case, we use the weight made of Tungsten. The density of Tungsten is 19.25 g/cm^3. The diameter and thickness of mass are 0.06m and 0.08 m, respectively. Therefore, the mass of the rotor mass is 4.485 kg. To measure this mass, we assumed that we use an electronic balance whose catalog number and accuracy are CG-6000 and 0.2 g, respectively. Therefore, the relative uncertainty of the mass of rotor mass is 0.04 %.

To make the rotor disk, we use the NC milling machine. The typical accuracy is less than 0.02 mm. For the measuring of the shape, we employ the three-dimension coordinate measuring machine (CMM).[33] The precision of CMM is 2 μm. We can measure the shape of the rotor and masses with enough of uncertainty using CMM.

The estimated relative uncertainties of the powers are 0.4%. One of the largest uncertainty is the geometrical factor of the Pcal laser. The geometrical factor uncertainty is assumed 0.3 %, which is same number of LIGO.

Finally, the estimated relative uncertainty of displacement is written as

$$\begin{aligned}\left(\frac{\delta x}{x}\right)^2 \quad &\sim \quad \left(\frac{\delta G}{G}\right)^2 + \left(\frac{\delta V_{in}}{V_{in}}\right)^2 + \left(\frac{\delta M}{M}\right)^2 + \left(\frac{\delta s(\omega)}{s(\omega)}\right)^2 + 25\left(\frac{\delta m_{\mathrm{q}}}{m_{\mathrm{q}}}\right)^2 + 16\left(\frac{\delta m_{\mathrm{h}}}{m_{\mathrm{h}}}\right)^2 \\ &+ \quad 25\left(\frac{\delta V_{2\mathrm{f}}^{\mathrm{R}}}{V_{2\mathrm{f}}^{\mathrm{R}}}\right)^2 + 16\left(\frac{\delta V_{2\mathrm{f}}^{\mathrm{R}}}{V_{2\mathrm{f}}^{\mathrm{R}}}\right)^2 + 100\left(\frac{\delta r_{\mathrm{q}}}{r_{\mathrm{q}}}\right)^2 + 144\left(\frac{\delta r_{\mathrm{h}}}{r_{\mathrm{h}}}\right)^2 .\end{aligned} \tag{33}$$

The contribution of the radius uncertainty is amplified by the O(100) factor. To reduce the noise of displacement, we need to reduce the uncertainty of the shape of the rotor and masses. The uncertainty of the $V_{2\mathrm{f}}^{\mathrm{R}}$,$V_{3\mathrm{f}}^{\mathrm{R}}$, V_0^{R} are much less than other contributions.We can reduce the uncertainty of these values with long time integration time due to the statistics. Each the uncertainty is listed in Table. 2. The estimated total uncertainty of the displacement is 0.3 %.

6. CONCLUSION

Photon calibrator is one of the powerful calibrators in advanced LIGO, advanced Virgo and KAGRA. It can calibrate the response of IFO and its uncertainty is essential for estimation of gravitational wave source. In

particular, the distance of the source is strongly depend on the absolute laser power of the photon calibrator. In previous study, the Gold standard, which response is calibrated by the laser power standard of NIST, is used for the absolute laser power calibration of the photon calibrator. However, current limit of the absolute laser power between each country is about 3.5 %. It is directly propagate to the uncertainty of absolute displacement of gravitational wave detector.

To solve the problem, we proposed the combination method of photon calibrator and gravity field calibrator. Gravity field calibrator can modulate the mirror using gravity gradient. By canceling the displacement of the test mass using the photon calibrator, we can calibrate the absolute laser power and displacement of the photon calibrator with accuracy of 0.4 % and 0.3 %.

This method has an advantage of a direct comparison of the amplitude of injected power and gravity field. In previous study, we need to consider the uncertainty of the optical efficiency through the window and mirrors. This is because we put the working standard at the outside of the chamber. However, the method of gravity field can compare the displacement directly. By using this method, we can calibrate the uncertainty of optical efficiency and absolute power of the laser. When we compare the laser power between each institute, we need to bring the working standard. However, we can try the absolute calibration using this method. As we mention about a few percent of the absolute uncertainty of laser in each country. The estimated uncertainty of the power of this method is 0.4%. It imply that we can make a new power standard using interferometer.

ACKNOWLEDGMENTS

We thank Rechard Savage, Darkhan Tuyrnbayev for discussion of the photon calibrator. We would like to express our gratitude to Prof.Takaaki Kajita and Prof.Henry Wong. We would like to thank the KEK Cryogenics Science Center for the support. YI was supported by Academia Sinica under Grants No. CDA-105-M06 in Taiwan. This work was supported by JSPS KAKENHI Grant Numbers 17H106133 and XXXXXX. This work was supported by MEXT, JSPS Leading-edge Research Infrastructure Program, JSPS Grant-in-Aid for Specially Promoted Research 26000005, MEXT Grant-in-Aid for Scientific Research on Innovative Areas 24103005, JSPS Core-to-Core Program, A. Advanced Research Networks, and the joint research program of the Institute for Cosmic Ray Research, University of Tokyo.

REFERENCES

[1] Abbott, B. P. et al., "Observation of gravitational waves from a binary black hole merger," *Phys. Rev. Lett.* **116**, 061102 (Feb 2016).

[2] Collaboration, T. L. S., "Advanced ligo," *Classical and Quantum Gravity* **32**(7), 074001 (2015).

[3] Acernese, F. et al., "Advanced virgo: a second-generation interferometric gravitational wave detector," *Classical and Quantum Gravity* **32**(2), 024001 (2015).

[4] Somiya, K., "Detector configuration of kagra–the japanese cryogenic gravitational-wave detector," *Classical and Quantum Gravity* **29**(12), 124007 (2012).

[5] Aso, Y., Michimura, Y., Somiya, K., Ando, M., Miyakawa, O., Sekiguchi, T., Tatsumi, D., and Yamamoto, H., "Interferometer design of the kagra gravitational wave detector," *Phys. Rev. D* **88**, 043007 (Aug 2013).

[6] "Gw170817: Observation of gravitational waves from a binary neutron star inspiral," *Physical Review Letters* **119**(16) (2017).

[7] Abbott, B. P. et al., "A gravitational-wave standard siren measurement of the Hubble constant," *Nature* **551**(7678), 85–88 (2017).

[8] Schutz, B. F., "Determining the hubble constant from gravitational wave observations," *Nature* **323**, 310–311 (Sep 1986).

[9] Holz, D. E. and Hughes, S. A., "Using gravitational- wave standard sirens," *The Astrophysical Journal* **629**, 15–22 (Aug 2005).

[10] Nissanke, S., Holz, D. E., Hughes, S. A., Dalal, N., and Sievers, J. L., "Exploring short gamma-ray bursts as gravitational-wave standard sirens," *The Astrophysical Journal* **725**, 496–514 (Nov 2010).

[11] Feeney, S. M., Peiris, H. V., Williamson, A. R., Nissanke, S. M., Mortlock, D. J., Alsing, J., and Scolnic, D., "Prospects for resolving the Hubble constant tension with standard sirens," (2018).

[12] Riess, A. G., Macri, L. M., Hoffmann, S. L., Scolnic, D., Casertano, S., Filippenko, A. V., Tucker, B. E., Reid, M. J., Jones, D. O., Silverman, J. M., and et al., "A 2.4constant," *The Astrophysical Journal* **826**, 56 (Jul 2016).

[13] Ade, P. A. R., Aghanim, N., Arnaud, M., Ashdown, M., Aumont, J., Baccigalupi, C., Banday, A. J., Barreiro, R. B., Bartlett, J. G., and et al., "Planck2015 results," *Astronomy and Astrophysics* **594**, A13 (Sep 2016).

[14] Clubley, D., Newton, G., Skeldon, K., and Hough, J., "Calibration of the glasgow 10 m prototype laser interferometric gravitational wave detector using photon pressure," *Physics Letters A* **283**(1), 85 – 88 (2001).

[15] Mossavi, K., Hewitson, M., Hild, S., Seifert, F., Weiland, U., Smith, J., Lück, H., Grote, H., Willke, B., and Danzmann, K., "A photon pressure calibrator for the geo 600 gravitational wave detector," *Physics Letters A* **353**(1), 1 – 3 (2006).

[16] Karki, S., Tuyenbayev, D., Kandhasamy, S., Abbott, B. P., Abbott, T. D., Anders, E. H., Berliner, J., Betzwieser, J., Cahillane, C., Canete, L., Conley, C., Daveloza, H. P., Lillo, N. D., Gleason, J. R., Goetz, E., Izumi, K., Kissel, J. S., Mendell, G., Quetschke, V., Rodruck, M., Sachdev, S., Sadecki, T., Schwinberg, P. B., Sottile, A., Wade, M., Weinstein, A. J., West, M., and Savage, R. L., "The advanced ligo photon calibrators," *Review of Scientific Instruments* **87**(11), 114503 (2016).

[17] Goetz, E., Jr, R. L. S., Garofoli, J., Gonzalez, G., Hirose, E., Kalmus, P., Kawabe, K., Kissel, J., Landry, M., O'Reilly, B., Siemens, X., Stuver, A., and Sung, M., "Accurate calibration of test mass displacement in the ligo interferometers," *Classical and Quantum Gravity* **27**(8), 084024 (2010).

[18] Goetz, E., Kalmus, P., Erickson, S., Jr, R. L. S., Gonzalez, G., Kawabe, K., Landry, M., Marka, S., O'Reilly, B., Riles, K., Sigg, D., and Willems, P., "Precise calibration of ligo test mass actuators using photon radiation pressure," *Classical and Quantum Gravity* **26**(24), 245011 (2009).

[19] "In preparation.,"

[20] Taylor, B. N. and Kuyatt, C. E., "Guidelines for evaluating and expressing the uncertainty of nist measurement results," tech. rep., NIST Tecnical Note 1297 (1994).

[21] Kuck, S., "Responsivity of detectors for radiant power of lasers, final report, edited by stefan kuck," *EUROMET Comparison Project* **156**, EUROMET.PR–S2 (2009).

[22] Forward, R. L. and Miller, L. R., "Generation and detection of dynamic gravitational- gradient fields," *Journal of Applied Physics* **38**(2), 512–518 (1967).

[23] Sinsky, J. and Weber, J., "New source for dynamical gravitational fields," *Phys. Rev. Lett.* **18**, 795–797 (May 1967).

[24] Sinsky, J. A., "Generation and detection of dynamic newtonian gravitational fields at 1660 cps," *Phys. Rev.* **167**, 1145–1151 (Mar 1968).

[25] H.Hirakawa, K.Tsubono, and K.Oide, "Dynamical test of the law of gravitation," *Nature* **283**(184) (1980).

[26] Oide, K., Tsubono, K., and Hirakawa, H., "The gravitational field of a rotating bar," *Japanese Journal of Applied Physics* **19**(3), L123 (1980).

[27] Suzuki, T., Tsubono, K., Kuroda, K., and Hirakawa, H., "Calibration of gravitational radiation antenna by dynamic newton field," *Japanese Journal of Applied Physics* **20**(7), L498 (1981).

[28] Ogawa, Y., Tsubono, K., and Hirakawa, H., "Experimental test of the law of gravitation," *Phys. Rev. D* **26**, 729–734 (Aug 1982).

[29] Kuroda, K. and Hirakawa, H., "Experimental test of the law of gravitation," *Phys. Rev. D* **32**, 342–346 (Jul 1985).

[30] Astone, P., Bassan, M., Bates, S., Bizzarri, R., Bonifazi, P., Cardarelli, R., Cavallari, G., Coccia, E., Degasperis, A., De Pedis, D., Frasca, S., Majorana, E., Merucci, L., Modena, I., Muratori, G., Pallottino, G. V., Patrignani, C., Pizzella, G., Price, M., Rapagnani, P., Ricci, F., and Visco, M., "Evaluation and preliminary measurement of the interaction of a dynamical gravitational near field with a cryogenic gravitational wave antenna," *Zeitschrift für Physik C Particles and Fields* **50**, 21–29 (Mar 1991).

[31] Matone, L., Raffai, P., Márka, S., Grossman, R., Kalmus, P., Márka, Z., Rollins, J., and Sannibale, V., "Benefits of artificially generated gravity gradients for interferometric gravitational-wave detectors," *Classical and Quantum Gravity* **24**(9), 2217 (2007).

[32] Tuyenbayev, D., Karki, S., Betzwieser, J., Cahillane, C., Goetz, E., Izumi, K., Kandhasamy, S., Kissel, J. S., Mendell, G., Wade, M., Weinstein, A. J., and Savage, R. L., "Improving ligo calibration accuracy by tracking and compensating for slow temporal variations," *Classical and Quantum Gravity* **34**(1), 015002 (2017).

[33] Inoue, Y. et al., "Two-layer anti-reflection coating with mullite and polyimide foam for large-diameter cryogenic infrared filters," (2016). [Appl. Opt.55,22(2016)].